

Spontaneous Lateral Composition Modulation in III-V Semiconductor Alloys

J. Mirecki Millunchick, R.D. Twesten, S.R. Lee, D.M. Follstaedt, E.D. Jones, S.P. Ahrenkiel, Y. Zhang, H.M. Cheong, and A. Mascarenhas

Introduction

The application of III-V semiconductor alloys in device structures is of importance for high-speed microelectronics and optoelectronics. These alloys have allowed the device engineer to tailor material parameters such as the bandgap and carrier mobility to the need of the device by altering the alloy composition. When using ternary or quaternary materials, the device designer presumes that the alloy is completely disordered, without any correlation between the atoms on the cation (anion) sublattice. However the thermodynamics of the alloy system often produce material that has some degree of macroscopic or microscopic ordering. Short-range ordering occurs when atoms adopt correlated neighboring positions over distances of the order of a few lattice spacings. This can be manifested as the preferential association of like atoms, as in clustering, or of unlike atoms, as in chemical ordering (e.g., CuPt ordering). Long-range ordering occurs over many tens of lattice spacings, as in the case of phase separation. In either short-range or long-range ordering, the band structure and the crystal symmetry are greatly altered.¹ Therefore it is absolutely critical that the mechanisms be fully understood to prevent ordering when necessary or to exploit it when possible.

Composition modulation is a subset

of phase separation. The term refers to the spontaneous formation of a phase-separated, self-organized periodic structure, as appears in Figure 1. Composition modulation in epitaxial growth has been observed to occur either parallel to (vertical modulation) or perpendicular to

(lateral modulation) the growth direction.¹ Vertical modulation has been observed in III-V materials such as InAsSb² and in II-VI materials such as ZnSeTe.³ Lateral modulation has been observed for a wide range of compound semiconductors during homogeneous growth,¹ when all components of the alloy are deposited simultaneously. This phenomenon has also been observed as a result of short-period superlattice growth,⁴⁻⁸ when alternating thin layers of each binary component of the alloy are deposited by molecular-beam epitaxy. The situation resulting from short-period superlattice growth is a particularly interesting case to study since the modulation is very strong and regular. This article will describe the microstructure and optical properties of lateral composition modulation in short-period superlattices, and will present a number of models proposing mechanisms for why it occurs in these films.

Microstructure

Lateral composition modulation in short-period superlattices shows similar microstructure over a range of material systems, including InP_m/GaP_n on GaAs,^{4,7} InAs_m/GaAs_n,^{5,6} and AlAs_m/InAs_n⁸ on InP (where *m* and *n* are the number of monolayers of each binary compound deposited). Figure 2a shows a cross-sectional dark-field transmission-electron-microscopy (TEM) micrograph with *g* = 002 of a compositionally modulated short-period superlattice of AlAs_{1,44}/

a) Short-Period Superlattice



b) Lateral Composition Modulation

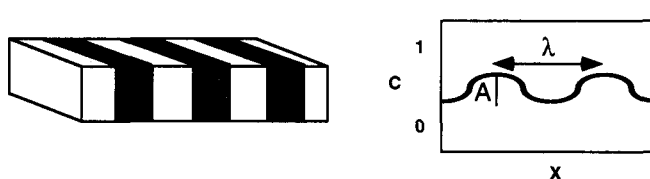


Figure 1. Schematic diagrams of the deposited and resulting structures. The upper figure (a) shows the as-deposited short-period superlattice with alternating layers along the growth direction *z*. The lower figure (b) shows the resulting compositionally modulated film. The average composition across such a modulated film varies along some crystallographic direction, in this case along *x*, with some characteristic modulation wavelength λ and amplitude *A*.

InAs_{1.56} in the [1 $\bar{1}$ 0] projection. The very strong and regular contrast variation across the film corresponds to modulation in composition. Figure 3a shows a corresponding x-ray reciprocal space map around the (224) reflection with the sample aligned such that the [1 $\bar{1}$ 0] direction is perpendicular to the diffraction plane, as recorded using Cu-K α x-rays and a position-sensitive detector.⁹ Distinct lateral satellites arising from composition modulation are visible on either side of the Bragg reflection of the short-period superlattice, with a wavelength of 180 Å. Typical modulation wavelengths range from 100 λ 200 Å, independent of material system, and are often predominantly aligned only along the [110] direction.⁴⁻⁸

Figures 2b and 3b show the complementary transmission electron micrograph and x-ray reciprocal space map of the same AlAs/InAs structure for the orthogonal crystallographic direction. These images show that lateral composition modulation in this material system is also present in the [1 $\bar{1}$ 0] direction with a wavelength of 330 Å. The amplitude of the composition modulation is more difficult to determine and varies greatly with the material system. The variation in the indium concentration for an InP/GaP short-period superlattice, for example, was reported to be greater than 20% by energy-dispersive x-ray spectroscopy.¹⁰

The anisotropy of the composition modulation can be explained by the difference in diffusion length in the two $\langle 110 \rangle$ directions, brought about by the surface reconstruction of the growth front. For a zinc-blende surface under group-V-rich conditions, the surface reconstruction is (2 × 4).¹¹ Theoretical calculations of a GaAs(001) surface, for example, show that group-III diffusion occurs along the [1 $\bar{1}$ 0] direction at a rate of approximately 100 times the rate along the [110] direction.¹² This anisotropy in the diffusion favors chemical segregation elongated in this direction. Reflection-high-energy-electron-diffraction (RHEED) patterns observed during InAs/GaAs short-period superlattice deposition show similar (2 × 4) reconstructions during InAs and GaAs deposition, resulting in composition modulation predominantly along the [110] direction. For the AlAs/InAs short-period superlattices on the other hand, the RHEED patterns change from (2 × 4) during the InAs deposition to (2 × 1) during the AlAs deposition.¹³ This change in surface reconstruction during growth is presumed to alter the diffusion kinetics of the surface.¹³ Subsequently, distinct

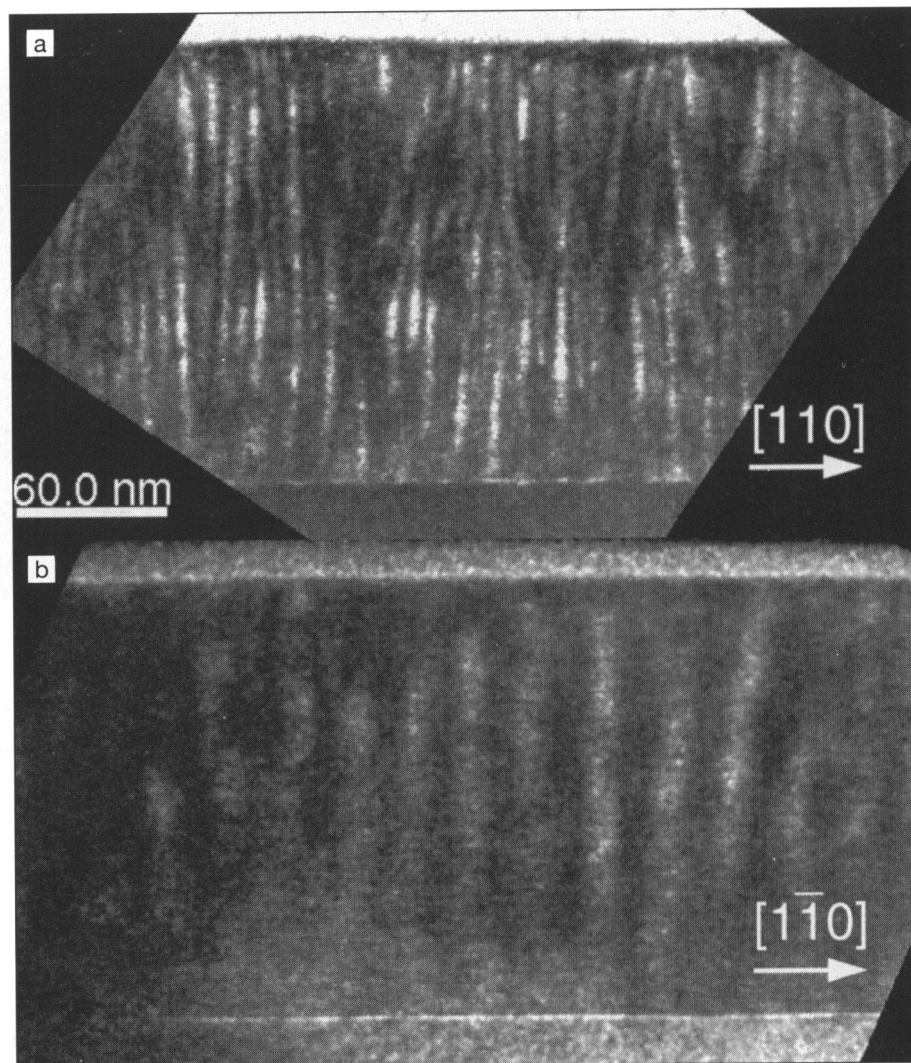


Figure 2. Dark-field cross-sectional transmission electron micrograph of an AlAs_{1.44}/InAs_{1.56} short-period superlattice with $g = 002$ in the (a) [110] and (b) [1 $\bar{1}$ 0] projections. The contrast variation across the sample corresponds to lateral composition modulation. The projected direction in the figure is normal to the page.

composition modulation is observed in both $\langle 110 \rangle$ directions in AlAs/InAs short-period superlattices.

If the surface reconstruction determines the fast and slow diffusion directions, varying the substrate miscut also alters the diffusion kinetics. By choosing a miscut angle toward the [110] direction, step edges are created parallel to the [1 $\bar{1}$ 0] direction, which suppress the fast diffusion in that direction by acting as an adatom sink. A study by Chen and co-workers⁴ of GaP/InP short-period superlattices deposited on 2° disoriented GaAs(001) substrates did not show any difference in the degree of composition modulation by TEM. However Yoshida and co-workers⁷ do report a dependence

of composition modulation on substrate misorientation angle for higher miscut substrates, most likely due to shorter terrace lengths.

The driving force for composition modulation in these structures is evident in higher magnification TEM micrographs. Figure 4 shows higher magnification bright-field $g = 002$ micrographs of two different InAs/AlAs short-period superlattices in the [1 $\bar{1}$ 0] projection. In addition to the lateral contrast due to composition modulation, contrast due to the individual short-period superlattice layers is also resolved. The structure in Figure 4a is nominally lattice-matched to the substrate. The superlattice layers are not flat; they are slightly corrugated. Fur-

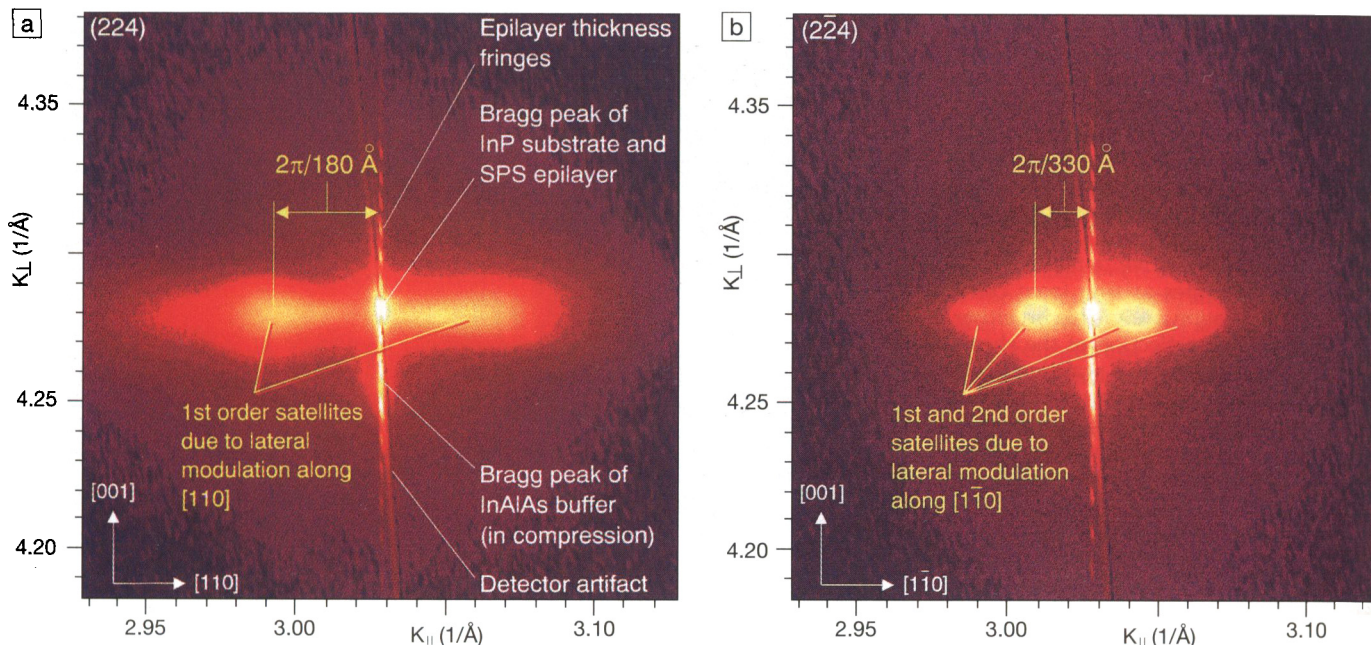


Figure 3. X-ray reciprocal space maps in the immediate vicinity of the (a) (224) and (b) (22̄4) reflections for an AlAs_{1.44}/InAs_{1.56} short-period superlattice. The lobes to either side of the short-period-superlattice Bragg peak reflect the lateral periodicity due to composition modulation with wavelengths of (a) $\lambda \sim 180$ Å along the [110] direction and (b) $\lambda \sim 330$ Å along the [110] direction.

thermore the corrugation is correlated with the lateral composition contrast. This effect is even more pronounced in the strained short-period superlattice structure (the average In composition of the superlattice layer is 46%) shown in Figure 4b. Here the layers are clearly cusplike in nature, with the notches of the cusps corresponding to an indium composition greater than 52%.⁸ In either case, the corrugated morphology and composition modulation were not observed until several periods of the short-period superlattice were deposited, indicating that these phenomena did not originate in the buffer layer but in the superlattice itself. This association of composition modulation with surface undulations has also been observed in homogeneously deposited II-VI alloys.^{14,15}

Theoretical Considerations

Although the formation of composition modulation is not fully understood, several models have been proposed. In an effort to understand experimental observations of lateral composition modulation, Glas calculated the elastic deformation and elastic energy of an epitaxial layer with a periodic variation in the lattice parameter and determined their effects on the thermodynamic stability of the film.¹⁶ He found that for a critical modulation wavelength of a

given film thickness, the elastic energy is minimized. The result is that the critical temperature for spinodal decomposition is higher than the coherent temperature calculated by Cahn.¹⁷ However this increase is not enough to destabilize these films at typical growth temperatures. Therefore it is unlikely that the observed composition modulation results from the decomposition of a homogeneous layer but rather that it occurs at the growth surface.

Cheng, Hsieh, and co-workers⁴⁻⁶ have made some valuable observations regarding the mechanisms of composition modulation in short-period superlattices. They have developed a model referred to as strain-induced lateral ordering (SILO) to explain how composition modulation is initiated. In most cases, composition modulation has been observed in superlattice structures where the constituent binary alloys are strain-balanced to the substrate. For example, InAs and GaAs are both approximately 3.5% lattice-mismatched with respect to InP(001), except that they are opposite in sign. In spite of the rather substantial misfit between the individual layers, a superlattice consisting of one or two integer monolayers of each binary compound is said to be strain-balanced, with a net strain within the structure of zero. Cheng and co-workers observed that composi-

tion modulation occurred when the short-period superlattice structure deviated slightly away from the strain-balanced condition. Composition modulation was not observed in samples of (GaAs)_m/(InAs)_n on InP substrates where $n = m = 1.0$ ML but was observed when n and m deviated from the integer value by approximately $\pm 5\%$.¹⁸ They postulated that the excess (deficient) adatoms of each deposited superlattice layer would nucleate islands (holes) at the growth front.⁴⁻⁶ The subsequent deposition of the other constituent binary would planarize the layer, but due to the strain field associated with buried islands,¹⁹ it can be shown that new islands (holes) will nucleate between the buried ones. (See Figure 5.) Thus composition modulation is initiated and continues throughout the growing film.

Although the nucleation-based SILO process may account for the initiation of composition modulation in short-period superlattices, it does not account for the observed surface undulations, modulation wavelengths, and modulation amplitudes. Therefore an additional mechanism must be at work. Linear stability analysis has shown that for a strained film a nonplanar surface is more stable than a flat one.²⁰ Consider for example a surface with an approximately sinusoidal surface corrugation, perhaps

initiated by the SILO process. The lattice can relax stress at the wave crests, but the stress is increased in the troughs, as shown in Figure 6. The change in strain energy across the surface results in a gradient in the surface diffusion, or chemical potential. In turn, material migrates from the trough to the crest, increasing the amplitude of the perturbation. The increase in surface energy due to roughening, on the other hand, tends to drive material from the crests to the troughs so that the amplitude of the corrugation is decreased. Thus there are competing mechanisms in the stability of the surface: The strain energy is destabilizing, and the interfacial energy is stabilizing.²¹ In the case of an alloy where the constituent species have a significantly varying atomic number, the surface undulation can result in composition modulation. In the presence of strain, the composition of the alloy will vary along the undulation direction because large atoms preferentially attach where the lattice is dilated with respect to the substrate and smaller atoms where the lattice is compressed,²¹ as illustrated in Figure 6.

The morphological instability model just described may be plausible, especially in light of the correspondence between morphology and composition modulation shown in Figure 4. There are difficulties with this analysis however. For example, effects due to surface reconstruction, surface steps, faceting, and interfaces are not addressed by this continuum model. Other models are being developed to accommodate these shortcomings. Srolovitz and co-workers are extending linear stability analysis for multilayer structures,²² and Tersoff has developed a framework that considers composition modulation during step-flow growth.²³

Optical Properties

Composition modulation is expected to have a number of interesting effects on optical properties. Photoluminescence spectroscopy performed on compositionally modulated short-period superlattices yields information on the band-edge states of the structure. By examining the polarization dependence of the emission, the extent of lateral confinement can be gauged. This is accomplished by a technique called polarized photoluminescence, which is similar to conventional photoluminescence with the addition of a polarization analyzer placed in front of the spectrometer and oriented either parallel or perpendicular to the composition-modulation direction.

Figure 7 shows a typical polarized-

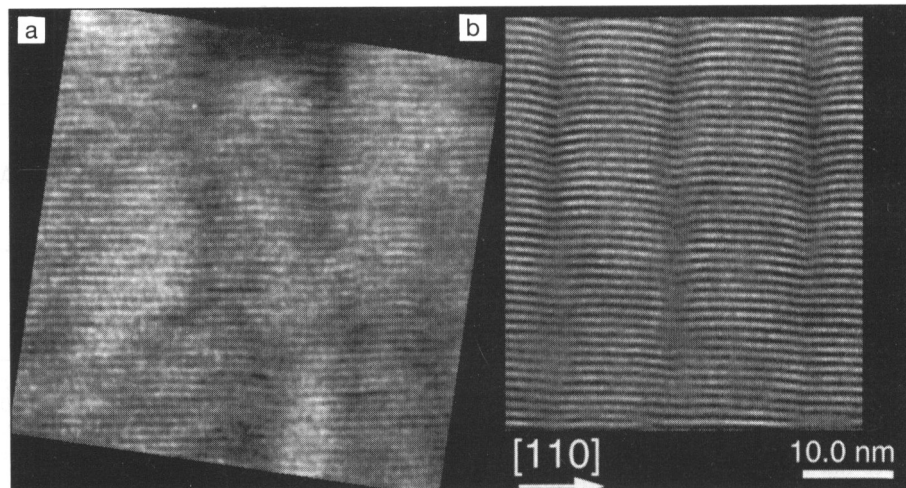


Figure 4. (a) High-magnification cross-sectional transmission electron micrograph in the $[1\bar{1}0]$ projection with $g = 002$ of a nominally lattice-matched $\text{AlAs}_{1.44}/\text{InAs}_{1.56}$ short-period superlattice that shows a slight undulation in the individual superlattice layers correlated to the composition-modulation contrast. (b) High-magnification cross-sectional transmission electron micrograph in the $[1\bar{1}0]$ projection with $g = 002$ of a $\text{AlAs}_{1.9}/\text{InAs}_{1.6}$ short-period superlattice under tension that shows a cusplike morphology of the individual superlattice layers, with the cusps positioned on the dark In-rich zones. The projected direction in the figure is normal to the page.

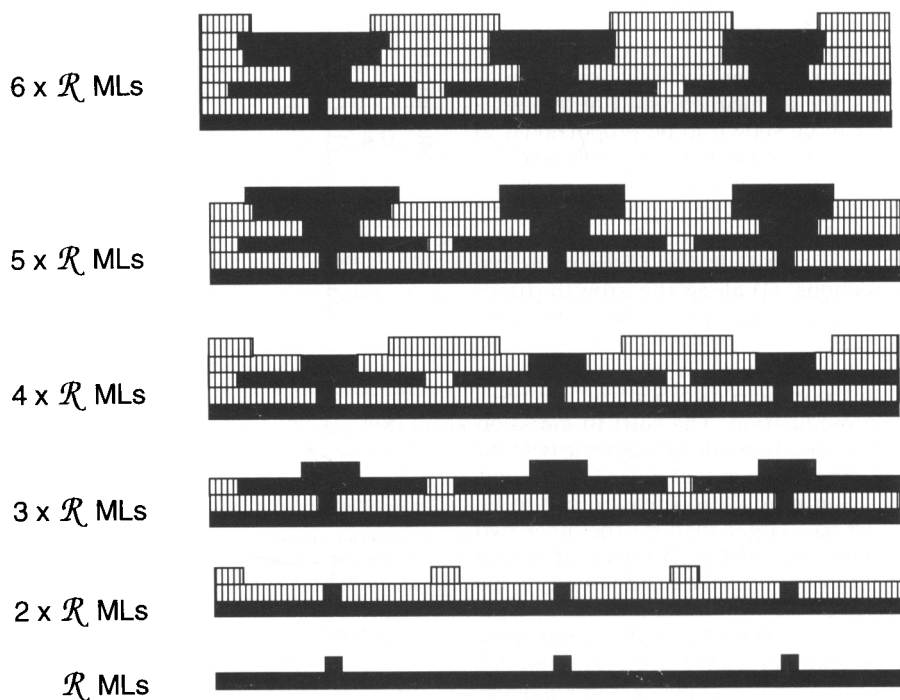


Figure 5. Schematic diagram illustrating a nucleation-based mechanism for the initiation of composition modulation in short-period superlattices. Composition modulation may be introduced by a noninteger number of monolayers per individual superlattice layer (denoted in the figure as \mathcal{R} MLs). The excess (deficient) atoms nucleate islands (holes) of one of the constituent binary alloys on the surface. Once these islands (holes) are buried by the subsequent superlattice layer, the resulting strain field will compel islands (holes) of the other constituent alloy to nucleate between the now-buried islands (holes).

photoluminescence spectrum taken at 8 K from a compositionally modulated InAs/GaAs short-period superlattice with a modulation wavelength $\lambda \sim 130 \text{ \AA}$. In this case, the emission energy occurs at 0.759 eV, with a polarization ratio of 10.3 to 1. In addition to the strong polarization, the emission energy itself is an important indicator of composition modulation. For a random alloy of InGaAs at the same average composition (In composition $x = 0.48$), the emission energy is expected to be 0.860 eV, 100-meV higher than the measured value. It is tempting to attribute this shift to radiative recombination in the lower bandgap In-rich regions. However such an assumption does not take into account the effects of strain and quantum confinement. Polarized emission can result from any effect that breaks the crystal symmetry of the film. Therefore other phenomena such as local ordering can also produce strong polarization of the emission energy,²⁴ making this measurement difficult to interpret explicitly.

Magnetoluminescence has been recently shown as an additional diagnostic tool to observe the presence of composition modulation.²⁵ In undoped semiconductors, a Coulomb interaction between the conduction-band electron and a valence-band hole can form a hydrogenic-type bound state, referred to as an exciton. From first-order perturbation calculations, the diamagnetic shift of this exciton can be shown to be proportional to the square of the magnetic field and inversely proportional to the cube of the reduced mass. The experiment is performed by measuring the exciton diamagnetic shift in the three principle directions: (1) along the growth direction, (2) perpendicular to the growth direction and parallel to the composition modulation, and (3) perpendicular to both the growth direction and composition modulation. The shift in emission energy as a function of magnetic field for the direction perpendicular to the composition modulation was found to be about 50% larger than for the other two orientations. Although the exact nature of the changes in the band structure due to composition modulation are not yet quantified, qualitatively the magnetoexciton shifts provide a good signature for the presence of composition modulation.

Conclusions

Lateral composition modulation in short-period superlattices has been shown to be very regular (with wavelengths $100 < \lambda < 400 \text{ \AA}$), strong (composition amplitudes $\pm 10\%$), and highly anisotropic (predominately aligned along

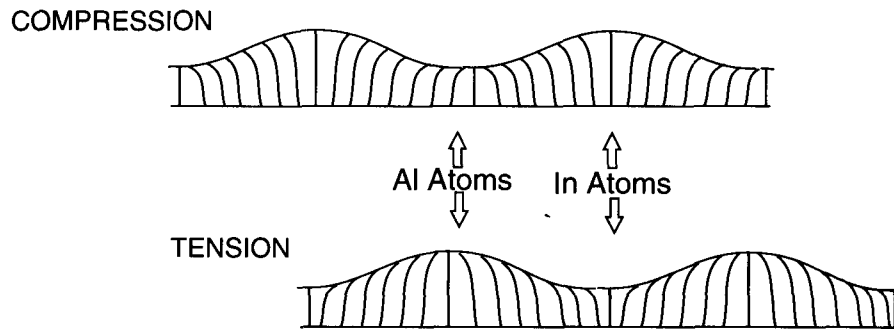


Figure 6. Schematic diagram illustrating how a strain-induced surface corrugation can initiate composition modulation for both compressive and tensile strains. Smaller atoms preferentially attach where the lattice is compressed, and larger atoms attach where it is dilated, thus initiating lateral composition modulation.

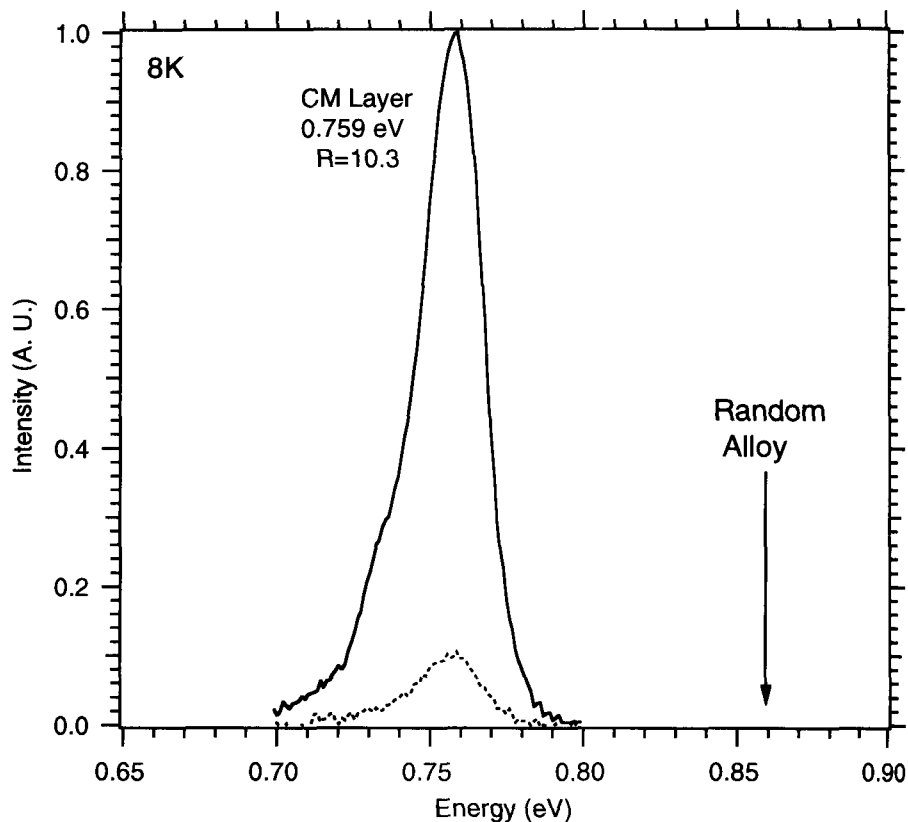


Figure 7. Typical photoluminescence spectra taken at 8 K for a compositionally modulated (CM) InAs/GaAs short-period superlattice. The emission energy is highly polarized and shifted to lower energy by 100 meV from the expected emission energy of a random alloy of the same composition (denoted by the arrow).

the [110] direction). There is evidence that the morphology of the growth front is strongly correlated to the composition modulation, suggesting that the morphological profile is related to composition modulation. These unique, spontaneous nanostructures modify the electronic

band structure and provide a new approach to band-structure engineering.

A variety of low-dimensional devices can benefit from lateral composition modulation. Quantum wells comprised of modulated material form quantum wires and dots, with carriers confined in

two or three directions. For example, light-emitting diodes and lasers²⁶⁻²⁸ with compositionally modulated active regions have already been fabricated. Low-dimensional laser structures have been shown to have lower threshold currents^{26,27} and temperature stability²⁸ than conventional quantum-well lasers.

Lateral composition modulation in short-period superlattices is just beginning to be understood. As this understanding grows, the device engineer will be able to exploit lateral composition modulation in device designs. With time the lessons learned from this phenomenon will be applied to the larger issues of alloy uniformity and ordering in general.

Acknowledgments

We wish to gratefully acknowledge the support of the U.S. Department of Energy, Office of Energy Research/Basic Energy Sciences Division of Materials Science Grant No. DE-AC02-83-CH10093.

References

1. A. Zunger and S. Mahajan, "Atomic Ordering and Phase Separation in Epitaxial III-V Alloys," in *Handbook of Semiconductors*, vol. 3, edited by T.S. Moss (Elsevier Science B.V., Amsterdam, 1994) p. 1399.
2. I.T. Ferguson, A.G. Norman, B.A. Joyce, T.R. Seong, G.R. Booker, R.H. Thomas, C.C.

- Phillips, and R.A. Stradling, *Appl. Phys. Lett.* **59** (1991) p. 3324.
3. S.P. Ahrenkiel, S.H. Xin, P.M. Reimer, J.J. Berry, H. Luo, S. Short, M. Bode, M. Al-Jassim, J.R. Buschert, and J.K. Furdyna, *Phys. Rev. Lett.* **75** (1995) p. 1586.
4. A.C. Chen, A.M. Moy, L.J. Chou, K.C. Hsieh, and K.Y. Cheng, *Appl. Phys. Lett.* **66** (1995) p. 2694.
5. S.T. Chou, K.Y. Cheng, L.J. Chou, and K.C. Hsieh, *J. Appl. Phys.* **78** (1995) p. 6270.
6. S.T. Chou, K.C. Hsieh, K.Y. Cheng, and L.J. Chou, *J. Vac. Sci. Technol. B* **13** (1995) p. 650.
7. J. Yoshida, K. Kishino, D.H. Jang, S. Nahm, I. Nomura, and A. Kikuchi, *Opt. Quantum Electron.* **28** (1996) p. 547.
8. J. Mirecki Millunchick, R.D. Twesten, D.M. Follstaedt, S.R. Lee, E.D. Jones, Y. Zhang, S.P. Ahrenkiel, and A. Mascarenhas, *Appl. Phys. Lett.* **10** (1997) p. 1402.
9. S.R. Lee, B.L. Doyle, T.J. Drummond, J.W. Medernach, and R.P. Schneider, Jr., in *Adv. in X-Ray Analysis*, edited by P.K. Predecki et al. (Plenum Press, New York, 1995) p. 201.
10. K.Y. Cheng, K.C. Hsieh, J.N. Baillargeon, and A. Mascarenhas, in *Proc. 18th Int. Symp. of GaAs and Related Compounds* (Inst. Phys. Conf. Ser. **120**, London, 1992) p. 589.
11. T. Hashizume, Q.K. Xue, J. Zhou, A. Ichimiya, and T. Sakurai, *Phys. Rev. Lett.* **73** (1994) p. 2208.
12. K. Shiraishi, *Appl. Phys. Lett.* **60** (1992) p. 1363.
13. J. Mirecki Millunchick, R.D. Twesten, S.R. Lee, D.M. Follstaedt, E.D. Jones, S.P. Ahrenkiel, Y. Zhang, H.M. Cheong, and A. Mascarenhas, *J. Electron. Mater.* in press.

14. G.C. Hua, N. Otsuka, D.C. Grillo, J. Han, L. He, and R.L. Gunshor, *J. Cryst. Growth* **138** (1994) p. 367.
15. S. Tomiya, H. Tsukamoto, S. Itoh, K. Nakano, E. Morita, and A. Ishibashi, (Materials Research Society, Pittsburgh, 1996) in press.
16. F. Glas, *J. Appl. Phys.* **62** (1987) p. 3201.
17. J.W. Cahn, *Acta Metall.* **9** (1961) p. 975.
18. K.Y. Cheng, K.C. Hsieh, and J.N. Baillargeon, *Appl. Phys. Lett.* **60** (1992) p. 2892.
19. Q. Xie, A. Madhukar, P. Chen, and N.P. Kobayashi, *Phys. Rev. Lett.* **75** (1995) p. 2542.
20. R.J. Asaro and W.A. Tiller, *Metal. Trans.* **3** (1972) p. 1789.
21. J.E. Guyer and P.W. Voorhees, *Phys. Rev. B* **54** (1996) p. 11710.
22. N. Sridhar, J.M. Rickman, and D.J. Srolovitz, *Acta Metall.* in press.
23. J. Tersoff, *Phys. Rev. Lett.* **77** (1996) p. 2017.
24. S.P. Ahrenkiel, R.K. Ahrenkiel, and D.J. Arent (Materials Research Society, Pittsburgh, 1996) in press.
25. E.D. Jones, J. Mirecki Millunchick, D.M. Follstaedt, M.J. Hafich, S.R. Lee, J. Reno, R.D. Twesten, Y. Zhang, and A. Mascarenhas, in *Proc. SPIE Int. Symp. On Optoelectronics* in press.
26. P.J. Pearah, A.C. Chen, A.M. Moy, K.C. Hsieh, and K.Y. Cheng, *IEEE J. Quantum Electron.* **30** (1994) p. 608.
27. A.M. Moy, A.C. Chen, K.Y. Cheng, L.J. Chou, K.C. Hsieh, and C.W. Tu, *J. Appl. Phys.* **80** (1996) p. 7124.
28. D.E. Wohlert, S.T. Chou, A.C. Chen, K.Y. Cheng, and K.C. Hsieh, *Appl. Phys. Lett.* **68** (1996) p. 2386. □



SYMPOSIUM TUTORIAL PROGRAM

Available only to meeting registrants, the tutorials will concentrate on new, rapidly breaking areas of research and are designed to encourage the exchange of information by meeting attendees during the symposium.

EXHIBIT

A major exhibit encompassing the full spectrum of equipment, instrumentation, products, software, publications, and services is scheduled for December 2-4 in the Boston Marriott and Westin Hotels convenient to the technical session rooms.

PUBLICATIONS DESK

A full display of over 500 books, plus videotapes and electronic databases, will be available at the MRS Publications Desk. Available at this meeting will be the MRS Symposium Proceedings from both the 1996 Fall and 1997 Spring Meetings, as well as the highly acclaimed *Handbook of Modern Ion Beam Materials Analysis*.

For additional meeting information or to request a detailed 1997 Fall Meeting Program, information on symposium tutorials, publications, or the Exhibit, contact:

MRS Member Services
9800 McKnight Road
Pittsburgh, PA 15237-6006
Telephone: 412-367-3004, Fax: 412-367-4373
E-mail: info@mrs.org
Website: <http://www.mrs.org/>

1997 FALL MEETING SYMPOSIA

- A: Evolution of Surface Morphology and Thin-Film Microstructure
- B: Phase Transformations and Systems Driven Far From Equilibrium
- C: Self-Organized Nanostructures
- D: Nitride Semiconductors
- E: Power Semiconductor Materials and Devices
- F: Infrared Applications of Semiconductors II
- G: Thin-Film Structures for Photovoltaics
- H: Materials and Devices for Si-Based Optoelectronics
- I: Semiconductors for Room-Temperature Radiation Detector Applications
- J: Electrical, Optical and Magnetic Properties of Organic Solid-State Materials IV
- K: Materials Science of the Cell
- L: Complex Fluids and Biomaterials
- M: Advances in Polymer Matrix Composites—Microscopic to Macroscopic
- N: Polymers in Confined Spaces
- O: Polymers in Orthopedics
- P: Modeling Across Length Scales for Materials Development
- Q: Semiconductor Process and Device Performance Modeling
- R: Tight-Binding Approach to Computational Materials Science
- S: Microscopic Simulation of Interfacial Phenomena in Solids and Liquids
- T: Stability of High-Temperature Superconductors—Robust Materials for Applications
- U: Ferroelectric Thin Films VI
- V: Metallic Magnetic Oxides
- W: Chemical Aspects of Electronic Ceramics Processing
- X: Frontiers of Materials Research
- Y: Materials for Electrochemical Energy Storage and Conversion II—Batteries, Capacitors and Fuel Cells
- Z: Recent Advances in Catalytic Materials
- AA: Covalently Bonded Disordered Thin-Film Materials
- BB: The Science and Technology of Thermal Spray Materials Processing
- CC: Particulate Coatings—Synthesis, Characterization and Related Fundamental Phenomena
- DD: High-Pressure Materials Research
- EE: Electrically Based Microstructural Characterization II
- FF: Surface-Controlled Nanoscale Materials for High-Added-Value Applications
- GG: Functionally Graded Materials
- HH: Materials Applications of Electron Holography and Related Techniques
- II: *In Situ* Process Diagnostics and Intelligent Materials Processing
- JJ: Nondestructive Characterization of Materials in Aging Systems
- KK: Atomistic Mechanisms in Beam Synthesis and Irradiation of Materials
- LL: High-Thermal-Conductivity Materials—Fundamentals and Applications
- MM: Advances in Materials for Cementitious Composites
- NN: Thin Films—Stresses and Mechanical Properties
- OO: Workshop on Materials Education

SPRING '97

1997 SPRING MEETING

MARCH 31- APRIL 4, 1997
SAN FRANCISCO, CALIFORNIA

These books are scheduled
for publication by fall or early
winter 1997.

Materials Research Society

9800 McKnight Road
Pittsburgh, PA 15237
Phone: 412-367-3012
Fax: 412-367-4373
E-mail: info@mrs.org

www.mrs.org/publications/books/forms/

The Newest Interdisciplinary Research on Advanced Materials

**1997 Spring Meeting
Symposium Proceedings**

**Place your order today for proceedings of the
1997 MRS Spring Meeting in San Francisco**

**A: Amorphous and Microcrystalline
Silicon Technology—1997**

Editors: E.A. Schiff, M. Hack, S. Wagner, R. Schropp,
I. Shimizu
ISBN: 1-55899-371-1 Code: 467-B
\$62.00 MRS Member
\$71.00 U.S. List
\$82.00 Non-U.S.

D: Gallium Nitride and Related Materials II

Editors: C.R. Abernathy, H. Amano, J.C. Zolper
ISBN: 1-55899-372-X Code: 468-B
\$62.00 MRS Member
\$71.00 U.S. List
\$82.00 Non-U.S.

**E: Defects and Diffusion in Silicon
Processing**

Editors: S. Coffa, T. Diaz de la Rubia, P.A. Stolk,
C.S. Rafferty
ISBN: 1-55899-373-8 Code: 469-B
\$65.00 MRS Member
\$75.00 U.S. List
\$86.00 Non-U.S.

**F: Rapid Thermal and Integrated
Processing VI**

Editors: T.J. Riley, J.C. Gelpey, F. Roozeboom,
S. Saito
ISBN: 1-55899-374-6 Code: 470-B
\$62.00 MRS Member
\$71.00 U.S. List
\$82.00 Non-U.S.

G: Flat Panel Display Materials III

Editors: R. Fulks, G. Parsons, D. Slobodin,
T. Yuzuriha
ISBN: 1-55899-375-4 Code: 471-B
\$62.00 MRS Member
\$71.00 U.S. List
\$82.00 Non-U.S.

**I: Polycrystalline Thin Films—Structure,
Texture, Properties and Applications III**

Editors: J. Im, S. Yalisove, B. Adams, Y. Zhu,
F-R. Chen
ISBN: 1-55899-376-2 Code: 472-B
\$65.00 MRS Member
\$75.00 U.S. List
\$86.00 Non-U.S.

**J: Materials Reliability in
Microelectronics VII**

Editors: J.J. Clement, J.E. Sanchez, Jr., K.S. Krisch,
Z. Suo, R.R. Keller
ISBN: 1-55899-377-0 Code: 473-B
\$65.00 MRS Member
\$75.00 U.S. List
\$86.00 Non-U.S.

L: Epitaxial Oxide Thin Films III

Editors: C. Foster, J.S. Speck, D. Schlom, C-B. Eom,
M.E. Hawley
ISBN: 1-55899-378-9 Code: 474-B
\$65.00 MRS Member
\$75.00 U.S. List
\$86.00 Non-U.S.

**M: Magnetic Ultrathin Films, Multilayers
and Surfaces—1997**

Editors: D.D. Chambliss, J.G. Tobin, D. Kubinski,
K. Barmak, W.J.M. de Jonge, T. Katayama, A. Schuhl,
P. Dederichs
ISBN: 1-55899-379-7 Code: 475-B
\$65.00 MRS Member
\$75.00 U.S. List
\$86.00 Non-U.S.

N: Low-Dielectric Constant Materials III

Editors: C. Case, P. Kohl, T. Kikkawa, W.W. Lee
ISBN: 1-55899-380-0 Code: 476-B
\$57.00 MRS Member
\$66.00 U.S. List
\$76.00 Non-U.S.

**P: Science and Technology of
Semiconductor Surface Preparation**

Editors: G.S. Higashi, M. Hirose, S. Raghavan,
S. Verhaverbeke
ISBN: 1-55899-381-9 Code: 477-B
\$60.00 MRS Member
\$68.00 U.S. List
\$79.00 Non-U.S.

**Q: Thermoelectric Materials—New
Directions and Approaches**

Editors: T.M. Tritt, G. Mahan, H.B. Lyon, Jr.,
M.G. Kanatzidis
ISBN: 1-55899-382-7 Code: 478-B
\$62.00 MRS Member
\$71.00 U.S. List
\$82.00 Non-U.S.

S: Materials for Optical Limiting II

Editors: P. Hood, R. Pachter, K. Lewis, J.W. Perry,
D. Hagan, R. Sutherland
ISBN: 1-55899-383-5 Code: 479-B
\$62.00 MRS Member
\$71.00 U.S. List
\$82.00 Non-U.S.

**Z: Specimen Preparation for Transmission
Electron Microscopy of Materials IV**

Editors: R.M. Anderson, S.D. Walck
ISBN: 1-55899-384-3 Code: 480-B
\$54.00 MRS Member
\$62.00 U.S. List
\$71.00 Non-U.S.

Also New From MRS!

**Advanced Metallization and Interconnect
Systems for ULSI Applications in 1996**

Editors: R. Havemann, J. Schmitz, H. Komiyama,
K. Tsubouchi
ISBN: 1-55899-385-1 Code: V12-B
\$58.00 MRS Member
\$65.00 U.S. List
\$72.00 Non-U.S.